

## Suppression of Spin Projection Noise in Broadband Atomic Magnetometry

JM Geremia, John K. Stockton, and Hideo Mabuchi  
 Physics and Control & Dynamical Systems, California Institute of Technology, Pasadena CA 91125  
 Dated: January 18, 2019)

We demonstrate that quantum nondemolition (QND) measurement, combined with a suitable parameter estimation procedure, can improve the sensitivity of a broadband atomic magnetometer by reducing uncertainty due to spin projection noise. Furthermore, we provide evidence that real-time quantum feedback control offers robustness to classical uncertainties, including shot-to-shot atom number fluctuations, that would otherwise prevent quantum-limited performance.

PACS numbers: 07.55.Ge, 03.65.Ta, 42.50.Lc, 02.30.Yy

Atom magnetometers estimate the magnitude of an external magnetic field by observing Larmor precession in a spin-polarized atomic sample [1]. A canonical procedure for "detecting" a magnetic field oriented along the  $y$ -axis (in a laboratory-fixed coordinate system) operates by aligning the magnetic moments of  $N$  spin- $\frac{1}{2}$  atoms along the  $x$ -axis. The resulting polarized atomic state is characterized by its net magnetization,  $\mathbf{F} = \hat{\mathbf{F}} \hat{\mathbf{i}}$ , where the quantum operator,  $\hat{\mathbf{F}}$ , corresponds to the total angular momentum of the collective atomic system.

Under the influence of the field,  $\mathbf{b} = B \hat{\mathbf{y}}$ , the atomic magnetization precesses from its initial value,

$$d\mathbf{F}(t) = -(\mathbf{F}(t) \cdot \mathbf{b}) dt; \quad \mathbf{F}(0) = h\mathbf{F}\hat{\mathbf{x}}; \quad (1)$$

where  $\mathbf{F} = N \mathbf{f}$  for  $N$  spin- $\frac{1}{2}$  atoms and the Larmor frequency,  $\omega_L = B$ , is determined by the gyromagnetic ratio,  $\gamma$ . These dynamics connect the mean spin vector to the  $xz$ -plane such that, in the small-time (and small-decoherence) limit appropriate for discussing detection thresholds, the  $z$ -component of the atomic magnetization is given by  $F_z(t) = B F_z(0) e^{-\gamma_L t}$ .

The magnetic field can thus be inferred from the slope of  $F_z$  during its small-angle Larmor precession,

$$\tilde{B} = \frac{1}{F} \frac{F_z(t)}{t} = \frac{1}{F} F_z^0; \quad 0 < t < \tau; \quad (2)$$

Uncertainty in the field estimation,  $\tilde{B}$ , results from various sources of error that can be divided into three classes: (1) spin projection noise [2], or quantum uncertainty in the initial orientation of  $\mathbf{F}$  due to non-commutativity of the quantum operators,  $F_x, F_y$  and  $F_z$ , (2) finite signal-to-noise in the physical measurement used to determine  $F_z$ , and (3) classical parameter uncertainties in Eq. (2), namely fluctuations in  $F$  that arise from shot-to-shot variance in the atom number,  $N$ .

Here we demonstrate that, given a quantum nondemolition (QND) measurement of  $F_z$  with a finite signal-to-noise ratio, degradation of the field sensitivity due to projection noise can be minimized by an estimation procedure [3, 4] that exploits the spin-squeezing produced by the QND measurement [5, 6, 7]. However, we find that the simplest procedure for suppressing spin projection

noise is susceptible to classical parameter uncertainty. Incorporating real-time quantum feedback control into the estimation procedure alleviates this source of error.

We consider a QND measurement of  $F_z$  performed by quantum-limited detection of an optical field scattered by the atomic system [7, 8]. Such a measurement is described by the continuous photocurrent,

$$P(t) = \frac{1}{M} F_z(t) + \eta(t); \quad (3)$$

where the  $\eta(t)$  are Gaussian stochastic increments that reflect detection (optical) noise. The measurement strength,  $M$ , relates the mean value of the photocurrent to the  $z$ -component of the collective atomic spin [7].

Our procedure [3] based on quantum Kalman filtering [9, 10] estimates the magnetic field from the average slope,  $y^0(\tau)$ , obtained by regressing the QND photocurrent over the interval  $0 < t < \tau$ . Figure 1 schematically illustrates this procedure. Beginning from the spin-polarized state at  $t = 0$ , the measurement reveals both the slope due to (small-angle) Larmor precession and an offset due to the initial uncertainty in the orientation of  $\mathbf{F}$ . This spin projection noise offset is randomly distributed with variance  $\hat{F}_z^2(0) = F=2$  in an ensemble of measurement trajectories, according to the Heisenberg-Robertson relation,  $\hat{F}_y^2 \hat{F}_z^2 = \frac{1}{4} h^2 \hat{F}_{xij}^2$ . Freedom to absorb the non-zero value of  $F_z(0)$  into the regression intercept rather than the slope minimizes the impact of the quantum projection noise on the estimated field,  $\tilde{B}$ .

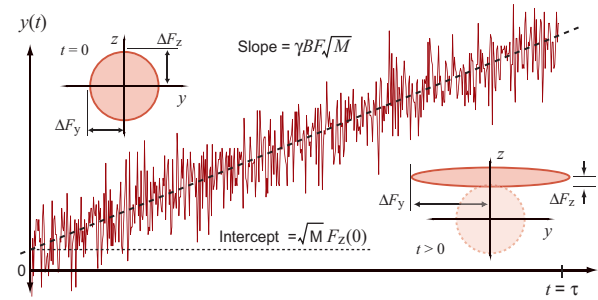


FIG. 1: Atomic magnetometry based on continuous QND measurement and quantum filtering enables field estimation procedures that suppress projection noise of the initial atomic state (simulated data).

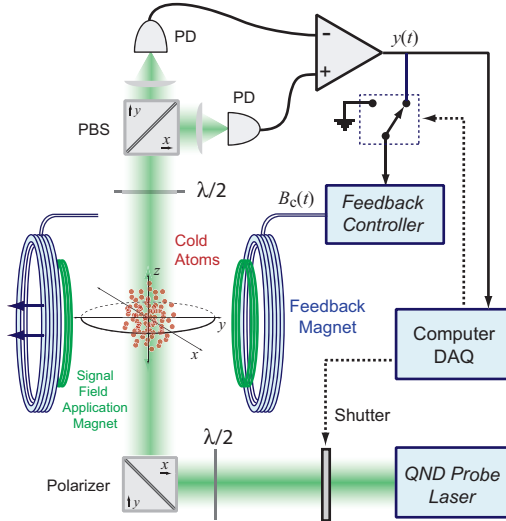


FIG. 2: Schematic of our apparatus for broadband atom magnetometry based on continuous QND measurement and real-time quantum feedback control.

Our single-shot magnetic field estimate is given by

$$\tilde{B}(t) = \frac{y^0}{F} \frac{1}{M}; \quad !_L^1; \quad (4)$$

where  $y^0$  is the photocurrent slope obtained by linear regression of  $y(t)$  over the time interval,  $0 \leq t \leq \tau$ . In principle, field uncertainty is limited only by statistical regression error  $\beta$ ,

$$\tilde{B}(t) = \frac{1}{F} \frac{\tau}{M} \frac{3}{\tau^2}; \quad (5)$$

where  $\mathbb{E}_{t=0}^{\tau} (t) dt^2$  is the integrated noise variance in a  $1/\tau$  bandwidth. The unitless QND signal to noise ratio,  $\text{SNR} = M = \beta$ , (both  $M$  and  $\beta$  have units proportional to frequency) is determined by experimental parameters, such as the optical probe power and detuning, and the scattering interaction strength [7].

The uncertainty of our optimal estimator, Eq. (5), should be compared to that of a procedure which cannot distinguish between Larmor precession and the initial spin projection noise. Such is the case for steady-state atom magnetometers [11, 12] where the uncertainty,

$$\tilde{B}(t) = \frac{2}{F} \frac{\tau}{M} \frac{F_z^2(0) + \frac{1}{M}}{\tau^2}; \quad (6)$$

retains a contribution from both  $F_z^2(0) = F=2$  and the optical shotnoise. In the limit of infinite signal to noise this expression saturates to the so-called shotnoise magnetometry limit [11]. Eq. (6) corresponds to an estimation procedure that averages the photocurrent,

$$\tilde{B}(t) = \frac{2}{F} \frac{\tau}{M} \frac{1}{\tau} \int_0^{\tau} y(t) dt; \quad (7)$$

rather than determining its slope. It is readily shown that steady-state atom magnetometers operate in a manner logically equivalent to this type of direct averaging.

Our estimation procedure, which suppresses projection noise, requires precise knowledge of the QND measurement sensitivity  $F/M$ . Shot-to-shot variation in  $N$  produces fluctuations,  $F$ , in the length of  $F$  that directly propagate into the field estimation as a proportional error,  $\tilde{B}_F = y^0 F = (F/M) \tilde{B} (F=F)$ . A similar argument applies to  $M$ . While relative parameter uncertainties introduce essentially no error when  $B=0$ , they can completely mask the improved resolution provided by spin-squeezing when  $B \neq 0$ .

To reduce the effects of classical parameter uncertainty, our magnetometer is implemented according to the closed-loop methodology [4] illustrated in Fig. 2. The QND photocurrent,  $y(t)$ , drives a precision y-axis magnet in negative feedback configuration to stabilize  $F_z$  to zero [8, 13]. In the presence of an external magnetic field, the controller imposes a compensating field,  $b_c(t) = B(t)y$  to prevent the atom magnetization from precessing out of the  $xy$ -plane. The magnetic field is estimated from the time-averaged feedback signal,

$$\tilde{B}(t) = \frac{1}{\tau} \int_0^{\tau} b_c(t) dt; \quad (8)$$

rather than the photocurrent. Since the magnetometer always operates with  $F_z = 0$ , the closed-loop estimation is reasonably immune to atom number fluctuations.

We have recently demonstrated QND detection and real-time quantum-limited feedback control with an apparatus similar to that in Fig. 2 [7, 13]. Our spin system is provided by the  $6^2S_{1/2}$  ( $F=4$ ) ground state hyperfine manifold in  $^{133}\text{Cs}$ . We obtain samples with  $N = 10^0 - 10^1$  atoms at a temperature of  $T = 10$  K via dark spontaneous-force optical trapping. Shot-to-shot fluctuations in  $N$  are  $< 20\%$ . Spin polarization along the  $x$ -axis is achieved by optical pumping on the  $6^2S_{1/2}$  ( $F=4$ )  $6^2P_{3/2}$  ( $F=4$ ) hyperfine transition and continuous QND measurement of  $F_z$  is implemented by balanced polarimetric detection of a laser detuned from the  $4^1S_1$  transition by  $\Delta = 550$  MHz.

Background magnetic fields are continually nulled using a combination of large (1 m) external three-axis Helmholz coils and smaller computer controlled trim-coils. The experiment is synchronized with respect to the 60 Hz line cycle, and we estimate the resulting shot-to-shot field fluctuations in a 100 s measurement window to be  $\sim 850$  nG. Atom decoherence is  $< 6\%$  over the  $t = 100$  s measurement trajectories we consider [7]. Further characterization of our state preparation, atom number, transverse spin relaxation, spin-squeezing, and quantum noise limited feedback performance can be found in Ref. [13]. A detailed procedure for determining the degree of atomic polarization and the QND signal to noise ratio can be found in Ref. [7].

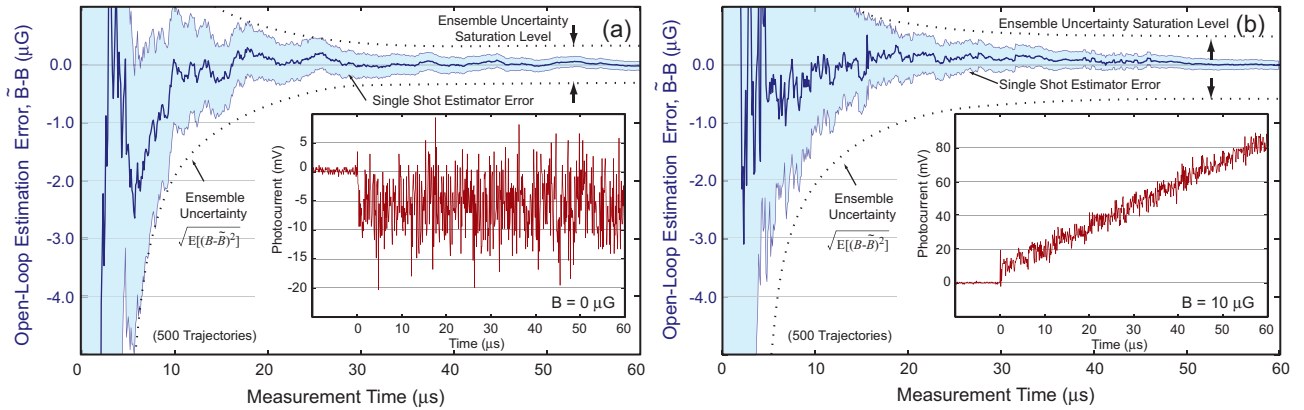


FIG. 3: Open-loop magnetic field estimation error,  $\tilde{B} - B$ , as a function of measurement time for (a)  $B = 0$  and (b)  $B = 10$  G. Inset plots show the Faraday polarimeter photocurrent for each QND measurement trajectory. The shaded regions indicate the single-shot regression uncertainty while the dotted curves reflect the ensemble error measured from 500 trajectories.

We began by operating our magnetometer with feedback disabled in order to characterize the adverse effects of classical parameter uncertainty. Fig. 3 shows example open-loop field estimations performed using the procedure in Eq. (4) for two different magnetic fields,  $B = 0$  and  $B = 10$  G. When the QND measurement is initiated at  $t = 0$  by opening the probe laser shutter [refer to Fig. 2] the photocurrent establishes an average offset [inset of Fig. 3(a)] that is randomly distributed in an ensemble of similar trajectories. Our ability to observe this random offset reflects sufficient signal-to-noise in our QND measurement to produce squeezing [3, 7, 13].

Since  $B = 0$  in Fig. 3(a), the atoms do not undergo Larmor precession and the slope of  $y(t)$  is, as expected,  $y^0 = 0$ . As described above, statistical fluctuations due to optical noise require that this slope be obtained by regression, as filtering the photocurrent reduces the sta-

tionary noise by time-averaging. The single-shot estimation trajectory for  $B = 0$  computed according to Eq. (4) is depicted by the dark solid line in Fig. 3(a) while the light shaded region denotes the single-shot field uncertainty,  $\tilde{B}$ , due to statistical error in the linear regression. Values for  $F$  and  $M$  needed to evaluate Eq. (4) were obtained from full-scale atomic Larmor precession according to the procedure detailed in Ref. [7].

The dotted lines in Fig. 3(a) indicate the ensemble field variance, computed as  $\mathbb{E}[(\tilde{B} - B)^2]^{1/2}$  from 500 QND trajectories, for the  $B = 0$  field estimate. At long times, this measure of the magnetometer performance saturates to the level of shot-to-shot background magnetic field fluctuations in our experimental apparatus, approximately 850 nG. However, prior to saturation, as depicted by the  $B = 0$  curves in Fig. 4, the regression estimation procedure (circles) outperforms the direct averaging estimator (triangles) given by Eq. (7). Unlike direct averaging, the regression estimator suppresses the uncertainty due to initial spin projection noise; the ensemble uncertainty drops below the field uncertainty threshold given by Eq. (6) [dotted line in Fig. 4].

It is important to note that the coherent state projection uncertainty (dotted line in Fig. 4) was computed using an absolute calibration [7] of  $M$ , and the average value of  $F$  inferred from full-amplitude Larmor precession measurements. Even though our optically pumped atomic system did not likely begin from a true minimum-uncertainty state due to imperfect pumping, sufficient QND spin noise reduction was achieved to allow the magnetometer to outperform the projection noise uncertainty corresponding to that of an actual coherent state.

In contrast, the  $B = 10$  G open loop estimation uncertainty fails to surpass the coherent state threshold despite a clearly visible photocurrent offset [inset in Fig. 3(b)] suggesting the presence of spin-squeezing. Evidently, the non-zero slope renders the open loop estimation susceptible to classical parameter uncertainty in  $F$  and  $M$ . As such, the long time estimation uncertainty

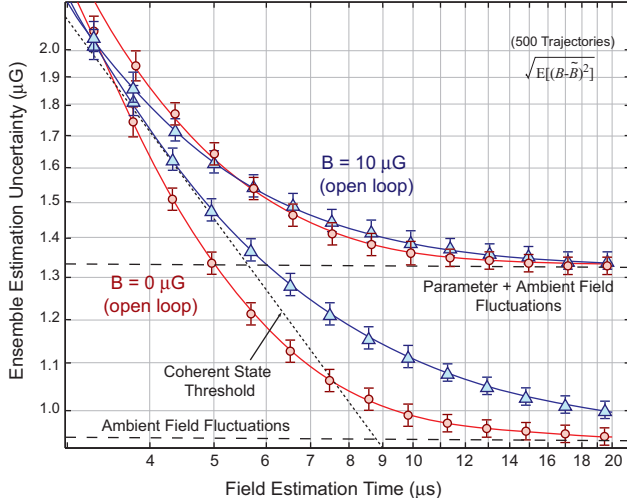


FIG. 4: Comparison of the two field estimation procedures, Eqs. (4) and (7) (circles and triangles, respectively) with  $B = 0$  and  $B = 10$  G. The dotted line reflects the theoretical sensitivity limit, Eq. (6), of a magnetometer with the same signal-to-noise ratio that does not exploit spin-squeezing.

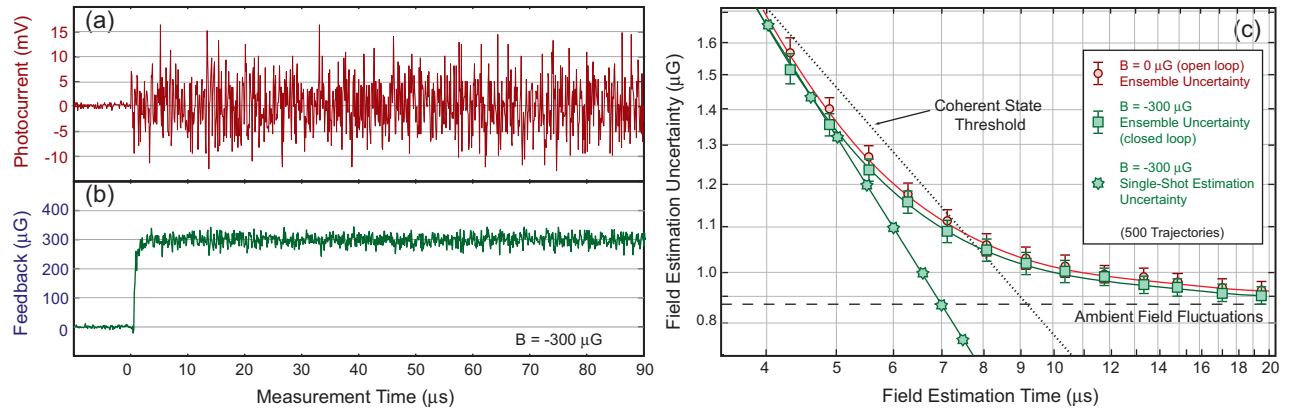


FIG. 5: (a) Closed-loop photocurrent for a  $B = -300 \mu\text{G}$  field, (b) realtime feedback field and (c) the resulting closed-loop field estimation error,  $B - B_c$ , as a function of measurement time.

for  $B = 10 \mu\text{G}$  saturates to a level much higher than that of the ambient magnetic field fluctuations, as in Fig. 4.

To alleviate the effects of classical parameter uncertainty, we next performed our closed-loop estimation procedure by enabling the feedback loop for the entire duration of each QND trajectory. The photocurrent in Fig. 5(a) displays no discernable slope despite the presence of a  $B = -300 \mu\text{G}$  field as the feedback loop drives a cancellation field [Fig. 5(b)],  $B_c$ , to maintain  $F_z = 0$ . The closed-loop field estimate, computed according to Eq. (8) for  $0 \leq t \leq 90 \mu\text{s}$ , is seen to be robust to shot-to-shot parameter fluctuations; it is evident from Fig. 5(c) that the ensemble uncertainty of the closed-loop estimator for  $B = -300 \mu\text{G}$  (squares) achieves similar performance to the  $B = 0$  open loop estimation (circles). Despite the large magnitude of the estimated field, the closed-loop procedure is able to outperform the coherent state projection noise threshold [dotted line in Fig. 5(c)].

It should also be pointed out that in closed loop configuration, where the estimation uncertainty is due almost entirely to QND detection noise, the ensemble variance is an overly conservative measure of the magnetometer performance. After all, ambient fluctuations that produce the 850 nG sensitivity error in Figs. 4 and 5(c) are real magnetic fields sensed by the atoms. Where other contributions to the detection threshold are well-controlled, the single-shot estimation error [Fig. 5(c) stars] more accurately reflects the magnetometer's performance. This single-shot closed-loop uncertainty surpasses the coherent spin state threshold at even long times in this case prior to the onset of significant atomic decoherence.

These results highlight what we anticipate will become a central theme in quantum-limited metrology. Feedback enables a precision measurement to achieve optimal insensitivity to classical uncertainty without sacrificing resolution [4, 14]. Furthermore, our closed loop methodology can be immediately extended to detection of non-stationary fields. Such an approach is likely to be essential for obtaining acceptable performance in various precision metrological applications including spin reso-

nance measurements, atomic frequency standards, and matter-wave gravimetry.

This work was supported by the NSF (PHY-9987541, EIA-0086038), the ONR (N00014-00-1-0479), and the Caltech MURIC center for Quantum Networks (DAAD19-00-1-0374). JK S acknowledges a Hertz fellowship. We thank Ramon van Handel, Andrew Berglund, Michael Armen, Andrew Doherty, David Budker and especially Daniel Leppner and Vladan Vuletic for helpful discussions.

Electronic address: jgeremia@caltech.edu

- [1] J. Dupont-Roc, S. Haroche, and C. Cohen-Tannoudji, Phys. Lett. A 28, 638 (1969).
- [2] W. Itano, J. Bergquist, J. Bollinger, J. Gilligan, D. Heinzen, F. Moore, M. Raizen, and D. Wineland, Phys. Rev. A 47, 3554 (1993).
- [3] JM Geremia, J. K. Stockton, A. C. Doherty, and H. Mabuchi, Phys. Rev. Lett. 91, 250801 (2003).
- [4] J. K. Stockton, JM Geremia, A. Doherty, and H. Mabuchi, Phys. Rev. A 69, 32109 (2004).
- [5] A. Kuzmich, L. Mandel, and N. P. Bigelow, Phys. Rev. Lett. 85, 1594 (2000).
- [6] B. Julsgaard, A. Kozhekin, and E. S. Polzik, Nature 413, 400 (2001).
- [7] JM Geremia, J. K. Stockton, and H. Mabuchi (2005), quant-ph/0501033 (note that the data presented in Ref. [7] was acquired after an overhaul of the apparatus utilized here and in Ref. [13]).
- [8] L. K. Thomsen, S. Mancini, and H. M. Wiseman, Phys. Rev. A 65, 061801 (2002).
- [9] V. P. Belavkin, Rep. on Math. Phys. 43, 405 (1999).
- [10] H. Mabuchi, Quantum Semiclass. Opt. 8, 1103 (1996).
- [11] D. Budker, W. Garroway, D. Kimball, S. Rochester, V. Yashchuk, and A. Weiss, Rev. Mod. Phys. 74, 1153 (2002).
- [12] I. K. Komiss, T. W. Komack, J. C. Allred, and M. Romanis, Nature 422, 596 (2003).
- [13] JM Geremia, J. K. Stockton, and H. Mabuchi, Science 304, 270 (2004).
- [14] D. W. Berry and H. M. Wiseman, Phys. Rev. A 65, 043803 (2002).